



Plasma Functionalized Scaffolds of Polyhydroxybutyrate Electrospun Fibers for Pancreatic Beta Cell Cultures

Emma Cortés-Ortiz¹, R. Olayo-Valles¹, Rogelio Rodríguez-Talavera², Maykel González-Torres³, Susana Vargas-Muñoz², R. Olayo¹, R. Godínez-Fernández⁴, Omar Eduardo Uribe Juárez⁴ and Juan Morales-Corona^{1*}

¹Departamento de Física, Universidad Autónoma Metropolitana, Unidad Iztapalapa, Mexico City, Mexico, ²Centro de Física Aplicada y Tecnología Avanzada, Universidad Nacional Autónoma de México, Santiago de Querétaro, México, ³Laboratorio de Biotecnología, Instituto Nacional de Rehabilitación Luis Guillermo Ibarra Ibarra, Ciudad de México, México, ⁴Departamento de Ingeniería Eléctrica, Universidad Autónoma Metropolitana, Unidad Iztapalapa, Mexico City, Mexico

OPEN ACCESS

Edited by:

Ana M. Beltrán,
University of Seville, Spain

Reviewed by:

Saeid Kargozar,
Mashhad University of Medical
Sciences, Iran
Sônia Maria Malmonge,
Federal University of ABC, Brazil
Paul Andrew Wieringa,
Maastricht University, Netherlands

*Correspondence:

Juan Morales-Corona
jmor@xanum.uam.mx

Specialty section:

This article was submitted to
Biomaterials,
a section of the journal
Frontiers in Materials

Received: 31 August 2020

Accepted: 19 February 2021

Published: 08 April 2021

Citation:

Cortés-Ortiz E, Olayo-Valles R, Rodríguez-Talavera R, González-Torres M, Vargas-Muñoz S, Olayo R, Godínez-Fernández R, Uribe Juárez OE and Morales-Corona J (2021) Plasma Functionalized Scaffolds of Polyhydroxybutyrate Electrospun Fibers for Pancreatic Beta Cell Cultures. *Front. Mater.* 8:600738. doi: 10.3389/fmats.2021.600738

Fibrous scaffolds based on biodegradable and biocompatible polyhydroxybutyrate (PHB) were produced by electrospinning. The scaffolds were coated by a thin solid film of polypyrrole, PPyl, deposited by plasma polymerization technique. FTIR and Raman spectroscopy results confirm the presence of PPyl on the PHB fibers, in FTIR can be show the signal of the NH₂ groups characteristic of the polypyrrole, so Raman show a broad band due to fluorescence from the PPyl coating. The morphology of the scaffolds was characterized by scanning electron microscopy, and the average fiber diameter of PHB is (2.68 ± 1.69) μm, also the average fibers diameter of PHB-PPyl is (3.57 ± 1.36) μm, the comparison of the average fibers diameter of coated and uncoated indicates that the average PPyl coated thickness is 0.45 μm. Crystallinity of the PHB fibers was characterized by X-ray diffraction and differential scanning calorimetry, the degree of crystallinity is estimated at 70%. Pancreatic beta cells (from the RIN-M cell line) were cultured on PHB and PHB-PPyl scaffolds. Cell viability results showed that the surface modified material is a good cell culture substrate for beta cells.

Keywords: plasma polymerization, polyhydroxybutyrate, electrospinning, scaffold, beta cells, tissue engineering

INTRODUCTION

Diabetes mellitus (DM) is a health problem that affects a substantial number of people all over the world. In 2019, 463 million people were estimated to have this disease. An important aspect in the development of this illness is the reduction of insulin producing pancreatic beta cells and their inability to produce enough insulin to control the glucose in blood (World Health Organization and International Diabetes Federation, 2006; De Fronzo et al., 2015; Ogurtsova et al., 2018). DM represents a serious public health problem with significant social and economic impact. For this reason, it is the subject of wide research. In search of an alternative to control and prevent DM, tissue engineering (TE) makes use of polymeric biomaterials combined with cells. One of the most important goals in this research field is the design of biomaterials that support cells and carry signaling molecules that allow tissue regeneration (O'Brien, 2011). TE scaffolds have been prepared from different biocompatible and biodegradable polymers

because of their easy processing. These polymers can be natural or synthetic, and scaffolds have been prepared from single polymers or combinations with other materials.

Polyhydroxyalkanoates are a family of biodegradable and natural polymers produced by microorganisms, used for biomedical applications. A member of this family of polymers is poly(3-hydroxybutyrate) (PHB). PHB exhibits biocompatibility, biodegradability, abrasion resistance, good mechanical strength, and adequate dimensional stability. Studies indicate that biodegradation of PHB is slower than poly(lactic acid), a commonly used biodegradable polymer (Zhuikov et al., 2021). PHB is a hydrophobic polymer with low cellular interaction, which limits its use in TE. PHB oligomers produced during degradation are non-toxic. The main disadvantage of PHB is its hydrophobic nature and lack of functional groups which results in low cell affinity, this limits its applications in TE. To solve the problem, PHB has been functionalized or mixed with other materials to create scaffolds that have good cellular interaction (Nahideh et al., 2019; Toloue et al., 2019; Naderi et al., 2020).

Various methods have been used for scaffold preparation, such as solvent casting, leaching, and electrospinning. One of the most widely used techniques is electrospinning, which can produce fibrous scaffolds with fiber diameters in the range from micrometers to nanometers. The fiber diameter can be controlled through the electrospinning process variables such as solution viscosity, applied voltage, injection flow rate, and needle-collector distance (Michael et al., 2001). The electrospun fibers have advantages for TE, such as high surface area, high porosity with interconnected pores that allow cell growth, proliferation, and differentiation in three dimensions (Sadeghi et al., 2016).

To improve biocompatibility, PHB has been electrospun with other materials, such as zinc oxide, (Zviagin Andrei et al., 2019), chitosan (Tolouea et al., 2019), carbon nanotubes, (Maryam and Saeed, 2020), and alumina nanowires (Tolouea et al., 2019). Degli Esposti and Chiellini, made bioactive and bioresorbable porous scaffolds for bone tissue regeneration, based on PHB and the incorporation of hydroxyapatite (Degli Esposti et al., 2019). Chondrocytes have been cultured on scaffolds of PHB/poly(hydroxybutyrate-co-hydroxyhexanoate) copolymer for cartilage regeneration (Ba et al., 2019). In the treatment of diabetic wounds, scaffolds of PHB with graphene oxide improved healing of normal and diabetic wounds (Daisy et al., 2020). PHB has also been combined with gelatin in electrospun scaffolds to evaluate their capability to treat diabetic wounds (Claudia et al., 2020).

One technique that has been shown to be effective in modifying the surface of different polymers is plasma polymerization. Surface modification can be accomplished by depositing a polymeric thin film that has functional groups that allow biomolecules to anchor to the surface (Ramírez-Fernández et al., 2012; Zuñiga Aguilar et al., 2014). Plasma polymerization using pyrrole as monomer has shown reliable performance in producing surfaces that promote cell adhesion and proliferation, especially in *in vivo* experiments (Ramírez-Fernández et al., 2015; Ruiz Velasco et al., 2017). Electrospun PHB has been treated by

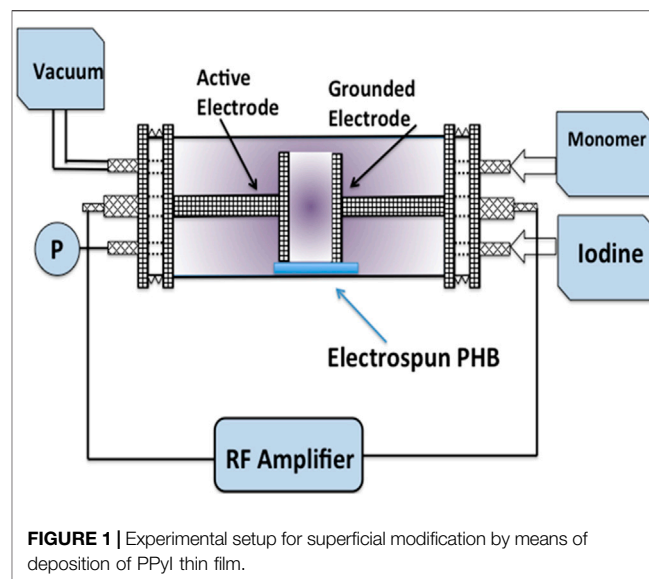


FIGURE 1 | Experimental setup for superficial modification by means of deposition of PPyI thin film.

plasma to improve its biocompatibility. Electrospun PHB scaffolds have been exposed to oxygen plasma discharge and polyaniline nanoparticles have been synthesized on the treated surface of the scaffolds. The results indicated that the modification by oxygen plasma and nanoparticles of polyaniline had a favorable impact on the cell adhesion and direction of cell growth (Zamanifard et al., 2020).

In this study PHB scaffolds were prepared by electrospinning. The diameter of the fibers in the scaffolds have nano and micrometer size, with a high area-to-volume ratio and pores with sizes in the micrometer range. The surfaces of the PHB fibers were modified by coating with a thin polymeric film of polypyrrole deposited by the plasma polymerization technique and doped *in situ* with iodine, PPyI. This film has the objective of improving the biocompatibility of the fiber. Structural analyses confirm the presence of PHB and PPyI in the coated scaffolds. The scaffolds were placed in beta cell culture and the results show that the PPyI coating produces a biologically active surface on the scaffolds.

EXPERIMENTAL

Materials

Poly(3-hydroxybutyrate) (product #363502, natural origin), pyrrole (product #131709, reagent grade, 98%), ethanol (product #459844, 200 proof, ACS reagent, $\geq 99.5\%$) and iodine (product #207772, ACS reagent, $\geq 99.8\%$) were purchased from Sigma-Aldrich, reactive grade chloroform (product #AC423550250, ACS reagent, $\geq 99.8\%$, Acros Organics) was purchased from Fisher Scientific, all substances were used without further purification.

PHB Electrospinning

PHB scaffolds were prepared in a NaBond Electrospinning United model TL-01 of Tong Li Tech (Shenzhen, China). The

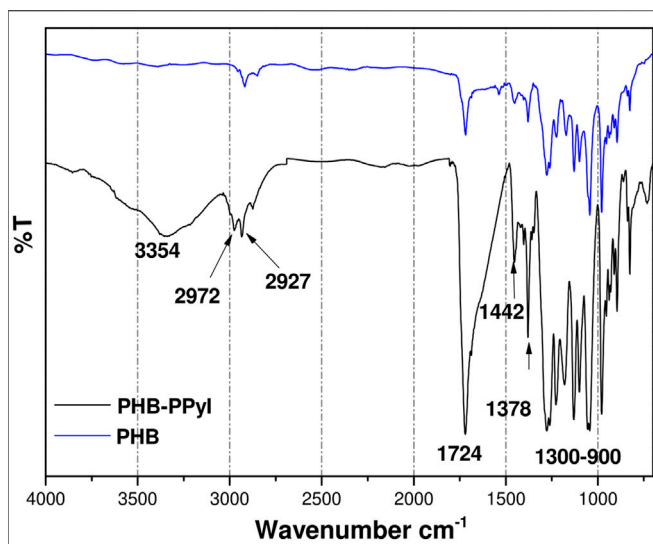


FIGURE 2 | FTIR spectra of PHB and PHB-PPyI scaffolds. Amine groups in PPyI produce the band at $3,354\text{ cm}^{-1}$.

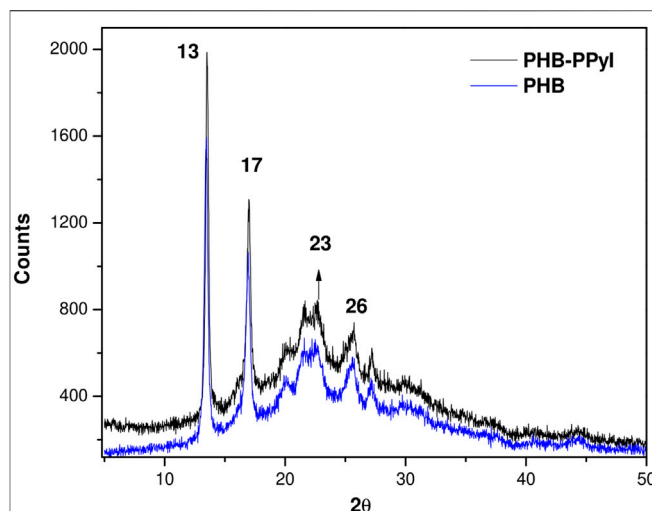


FIGURE 4 | X-ray diffractograms of PHB and PHB-PPyI. The lattice parameters of PHB and PHB-PPyI scaffold were $a = 5.65\text{ \AA}$, $b = 13.61\text{ \AA}$ and $c = 5.86\text{ \AA}$.

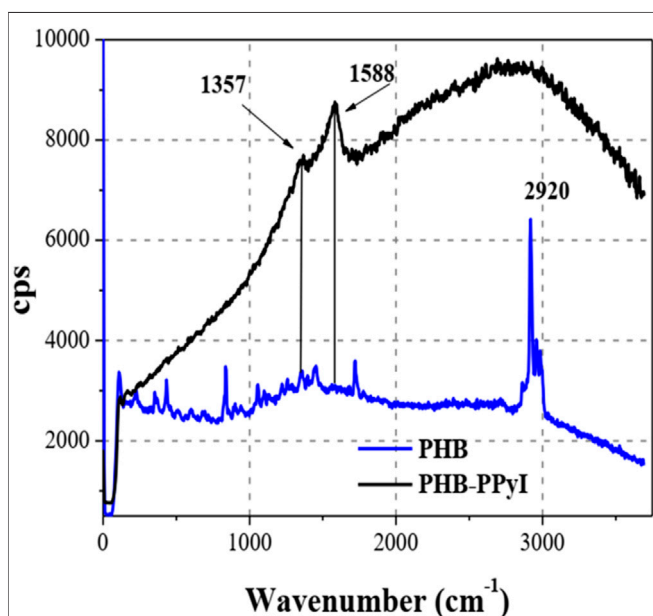


FIGURE 3 | Raman spectra of PHB and PHB-PPyI scaffolds. The broad signal in the PPyI spectrum is due to fluorescence.

machine is equipped with a 2-channel injection pump, a variable high-voltage source (0–30 kV) and a rotating cylinder collector 10 cm in diameter, with variable angular speed. In a typical experiment, PHB (1.2 g) was dissolved in 10 ml of a chloroform/ethanol mixture (9/1 v/v). The solution was heated to 50°C with stirring using a magnetic stirrer for 1 h. The solution was then introduced into a disposable syringe (20 ml) and placed in the injection pump. The injection flow rate was set to 3.0 ml/h. The solution was pushed through a food grade Teflon hose and reached a

0.6 mm ID needle. The collecting cylinder was covered with aluminum foil. A voltage of 15.0 kV was applied between the needle tip and the collector, and the needle-collector distance was set to 12 cm. PHB fibers were deposited on the collector, which was rotating at 1700 rpm. The electrospinning total time was 6.5 h.

PHB Surface Modification by Plasma Polymerization

Samples of PHB electrospun material were cut (approx. area of 1.0 cm^2) and placed inside a plasma reactor. The plasma reactor (Figure 1) consists of a Pyrex glass tube of 90 mm external diameter and 250 mm long. Each end of the tube was sealed with a stainless-steel flange. Stainless-steel rods fitted with a 70 mm plate on their end, were inserted through the center of each flange and placed 5 cm apart. Each flange has two access ports. One port was used to introduce the pyrrole monomer and the iodine dopant. Pyrrole and iodine were in separate reservoirs and were introduced into the plasma reactor in vapor form. A pirani pressure gauge (Edwards) and a vacuum system consisting of a cold trap and a mechanical vacuum pump (Edwards) were fitted on the other flange. Plasma polymerization was performed using 20 W of power, a pressure of 2×10^{-2} Torr, a total synthesis time of 30 min and rf of 13.56 MHz.

Characterization Raman Spectroscopy

Raman spectra of the scaffolds were obtained with a WiTec Raman System Alpha 300 RA confocal microscope. The samples were exposed to light from a 532 nm wavelength and 75 mW laser. Spectra were obtained from 32 replicate scans recorded between $3,700\text{ cm}^{-1}$ and 200 cm^{-1} with 4 cm^{-1}

TABLE 1 | PHB XRD signals.

Crystalline plane	(020)	(110)	(101)	(121)
2θ	13°	17°	23°	26°
d (Å)	6.80	5.21	3.56	3.42

resolution. Samples were placed on the Raman System stage without further treatment.

Infrared Spectroscopy

The PHB and PHB-PPyI scaffolds were characterized by Fourier transform infrared spectroscopy (Perkin-Elmer GX-2000 System) with an attenuated total reflectance unit (Smith diamond DuraSample II). Spectra was recorded with 64 scans between $4,000\text{ cm}^{-1}$ and 400 cm^{-1} with 4 cm^{-1} resolution.

X-Ray Diffraction

The crystalline structure of PHB and PHB-PPyI scaffolds were studied by X-ray diffraction with a Bruker D8 Advance ECO diffractometer equipped with SSD160 detector, and Cu K α X-ray source (0.15406 nm wavelength). Scaffold samples of 1 cm^2 were placed in the sample holder and the diffractograms were acquired in a 2θ range of 2° – 50° .

Differential Scanning Calorimetry

Differential scanning calorimetry was performed in a DSC instrument (DSC 2820 Modulated DSC, TA Instruments). Scaffold samples were placed in sealed aluminum trays. The samples were heated from 20 to 200°C using a $10^\circ\text{C}/\text{min}$ heating ramp and were then cooled at $10^\circ\text{C}/\text{min}$ from 200 to 20°C . The degree of crystallinity was calculated from the ratio of the enthalpy of fusion (ΔH_m) of the sample to the enthalpy of fusion of 100% crystalline PHB, $\Delta H_{0m} = 146\text{ J/g}$ (Barham et al., 1984).

Scanning Electron Microscopy

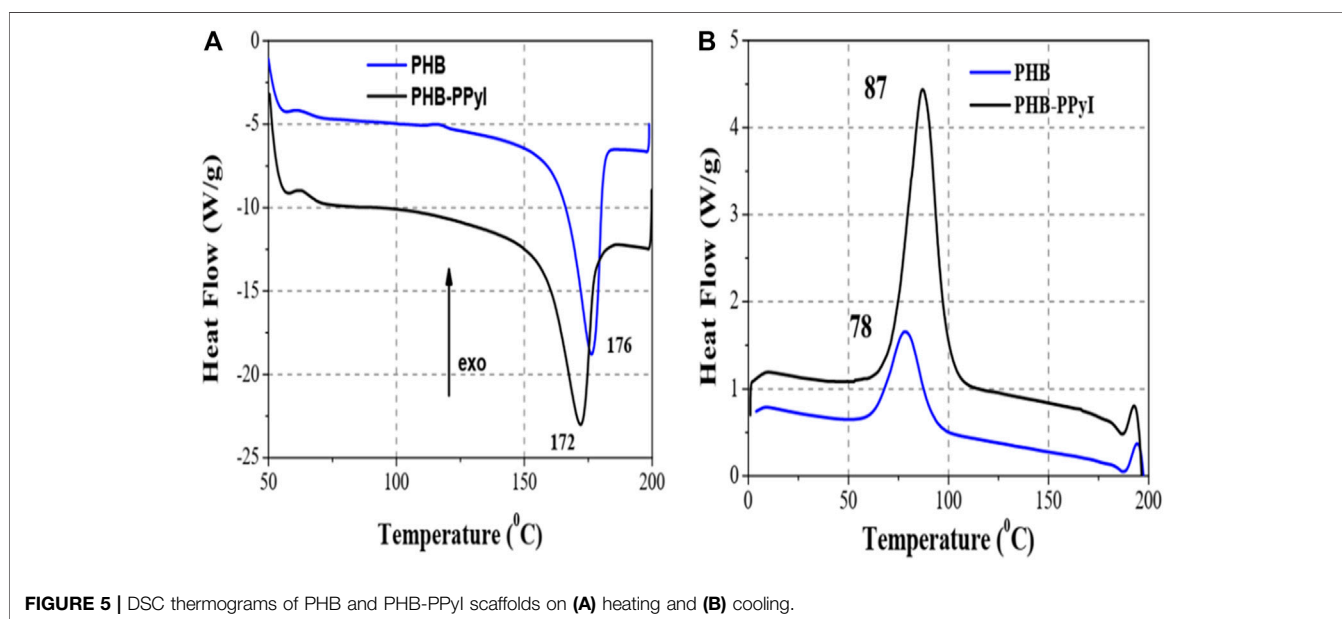
The morphology of the scaffolds was characterized from images obtained using a high-resolution scanning electron microscope (HRSEM JEOL JSM-7600F), at an accelerating voltage of 30 kV. The samples were coated by sputtering with a thin film of gold with 5 nm thickness, prior to SEM analysis. The fiber diameters were measured from SEM images using ImageJ software (National Institutes of Health, United States, version 1.53b). Histograms of fiber diameters were prepared and best fits to normal distribution were made using Origin software (OriginLab, version 8.1).

Cell Culture

Scaffold samples were sterilized overnight under UV light. Cells from the RIN-M cell line were cultured on the sterilized scaffolds. This cell line comes from a male rat's insulinoma of the Rattus Norvegicus species. The cells secrete insulin and somatostatin. They have an epithelial morphology and an approximate size of $10\text{ }\mu\text{m}$. Cells were proliferated following the ATCC® protocol using RPMI-1640 (ATCC® 30-2001) as the base culture medium and supplementing with fetal bovine serum and antibiotic with antimycotic at 10 and 1% of the total volume, respectively. The cells were incubated in a moistened environment with 5% CO_2 at 37°C , using $100 \times 20\text{ mm}$ culture petri dishes (product # CLS430167, Sigma Aldrich) and changing the culture medium every 3 days. The number of cells seeded on each scaffold was 4×10^4 .

Cell Viability

To determine cell viability, a Calcein-AM and Ethidium-1 Homodimer kit purchased from AccessoLab was used. The scaffolds were washed with PBS buffer for 5 min and the supernatant was removed, this process was repeated two times. A PBS solution with Calcein-AM and Ethidium Homodimer-1 was prepared with a concentration of 1 and $2\text{ }\mu\text{M}$, respectively. A volume of $500\text{ }\mu\text{l}$ of the solution was added to the scaffold

**FIGURE 5** | DSC thermograms of PHB and PHB-PPyI scaffolds on (A) heating and (B) cooling.

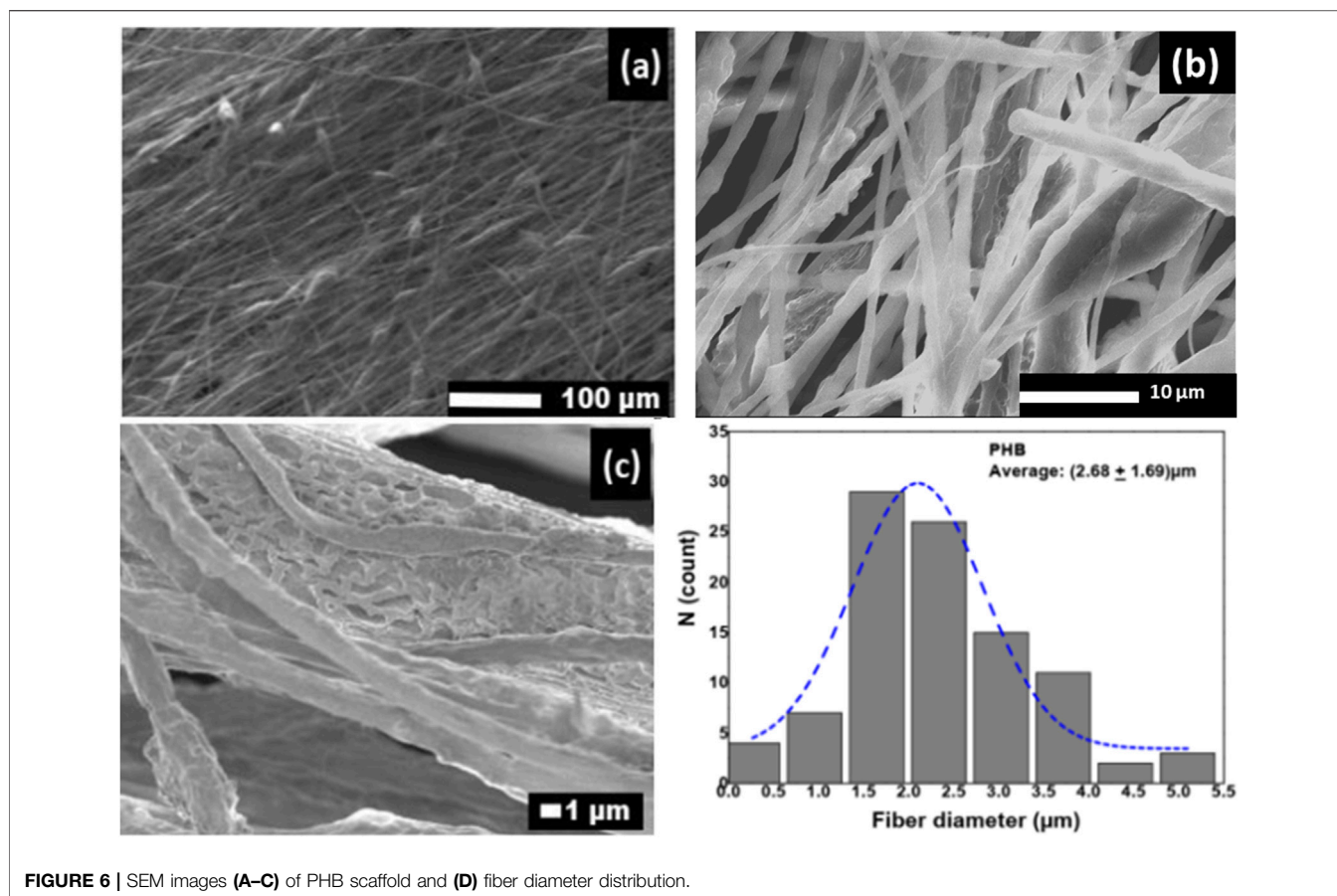


FIGURE 6 | SEM images (A–C) of PHB scaffold and (D) fiber diameter distribution.

samples. The samples were covered to protect them from light and allowed to stand before being viewed under the confocal microscope. With this technique, viable cells fluoresce green while dead cells fluoresce red.

RESULTS AND DISCUSSION

FTIR Analysis

The infrared spectra of uncoated PHB and surface-modified PHB-PPyI scaffolds are shown in Figure 2. The most intense band of the PHB is found at 1724 cm^{-1} , corresponding to the characteristic stretch of the carbonyl bond (ester carbonyl stretch). Peaks at $2,972\text{ cm}^{-1}$ and $2,927\text{ cm}^{-1}$ are characteristic of aliphatic CH_3 and CH_2 groups. The band at $1,442\text{ cm}^{-1}$ corresponds to the asymmetric deformation of C-H bonds, and the signal corresponding to stretching of these bonds is also observed at $1,378\text{ cm}^{-1}$. The series of intense bands located between 900 and $1,300\text{ cm}^{-1}$ correspond to the stretching of the C-O bond of the ester group. The spectrum of PHB-PPyI shows a broad and intense band between $3,100$ and $3,700\text{ cm}^{-1}$, this signal is due to amine groups along with hydroxy groups. Since this band is not present in the PHB spectrum, it is produced by vibrations of chemical groups in the PPyI coating. Also, in the PHB-PPyI spectrum, the band at 1724 cm^{-1} shows a shoulder

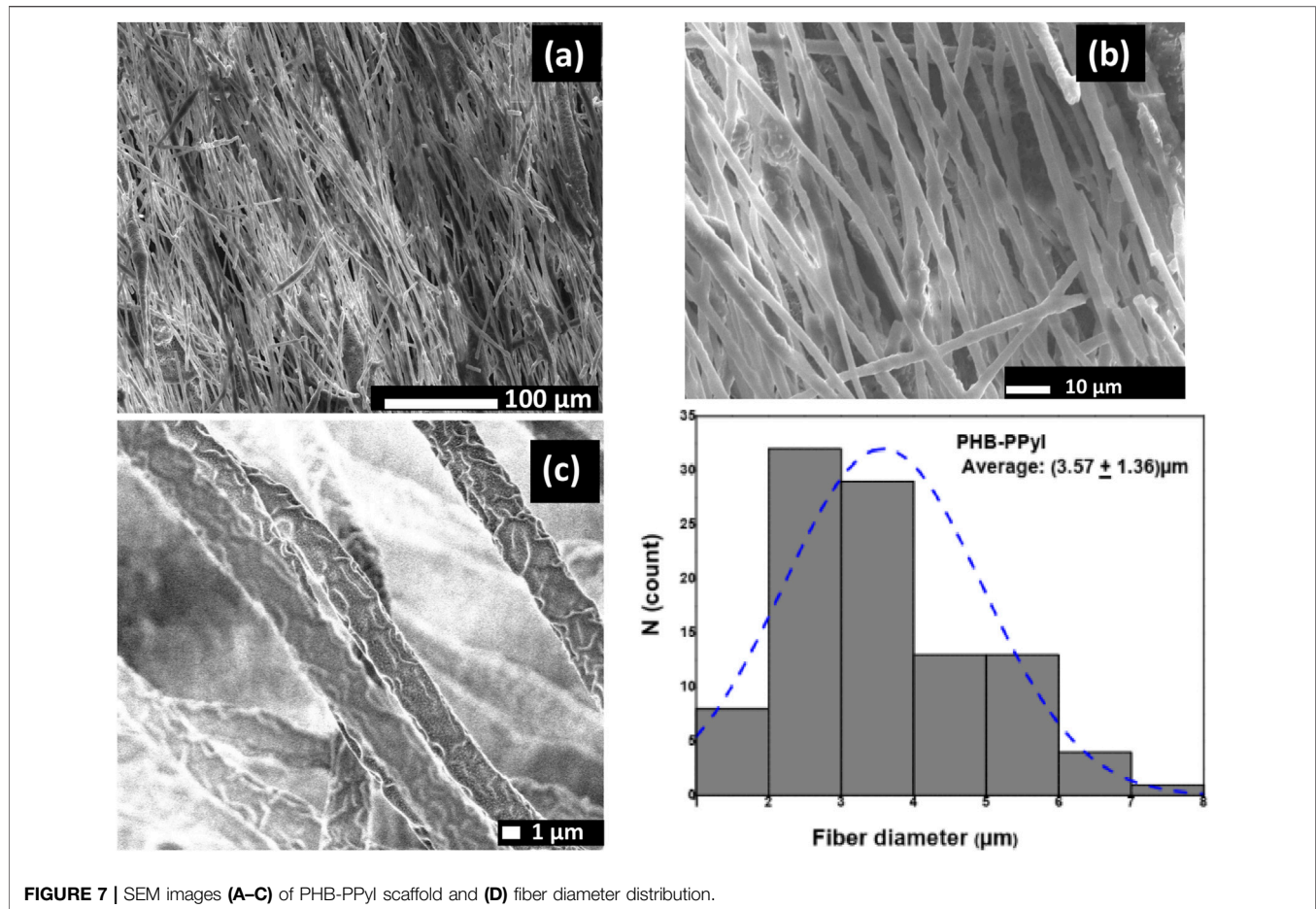
around $1,627\text{ cm}^{-1}$ which is due to amine groups in the PPyI coating (Zuñiga Aguilar et al., 2014).

Raman Spectroscopy

Raman spectra obtained with a Raman confocal microscope are shown in Figure 3. The Raman spectrum of the PHB scaffold shows an intense band at $2,920\text{ cm}^{-1}$ that corresponds to aliphatic carbons. The spectrum is consistent with other reports (Furukawa et al., 2006; Tsuyoshi et al., 2006). In contrast, the Raman spectrum of PHB-PPyI shows a broad band between $1,600$ and $3,600\text{ cm}^{-1}$ which masks most other signals. This broad band is due to fluorescence from the PPyI coating (Vazquez Ortega et al., 2014). Two other bands can be observed at $1,357$ and $1,588\text{ cm}^{-1}$. The first of these bands is likely due to aliphatic CH_3 groups and is also present in the PHB spectrum. The second band is only present in the PHB-PPyI spectrum and is likely due to the presence of iodine (Vazquez Ortega et al., 2014).

Crystalline Structure

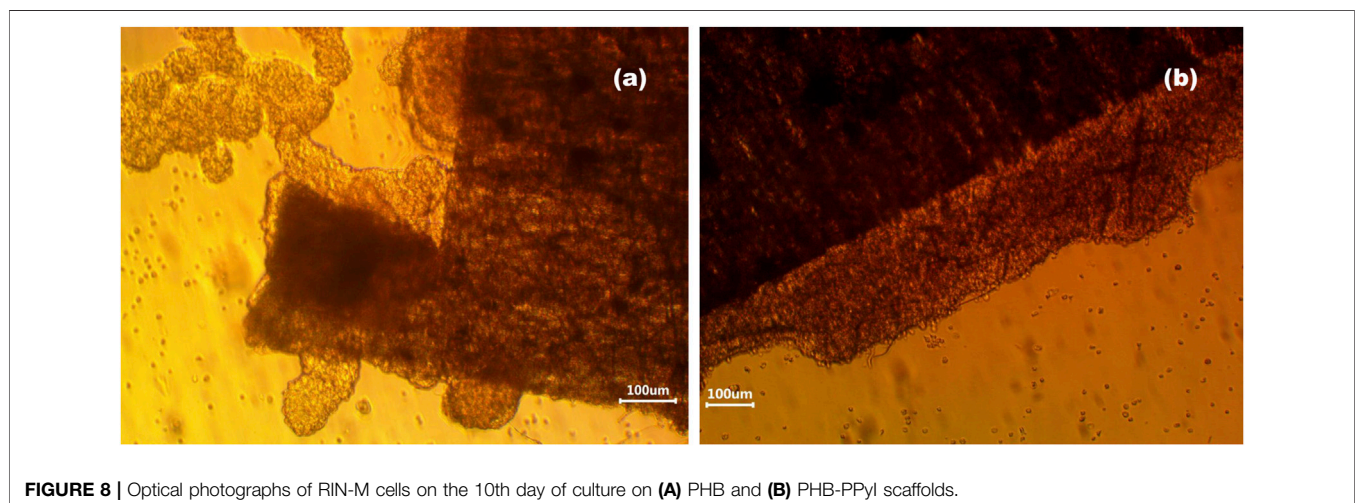
The X-ray diffractograms of PHB and PHB-PPyI were obtained at room temperature and are shown in Figure 4. Both samples present the same diffraction signals, showing that the PPyI surface coating did not affect the PHB crystallinity (Socrates, 2001). The figure shows two very intense diffraction peaks centered at $2\theta = 13^\circ$ and 17° corresponding to the (020) and (110) planes of the orthorhombic



unit cell of PHB crystals. Less intense diffractions are located around $2\theta = 23^\circ$ and 26° , corresponding to (101) and (121) planes, respectively (Tolouea et al., 2019).

PHB crystals have an orthorhombic unit cell with dimensions $a = 5.76 \text{ \AA}$, $b = 13.20 \text{ \AA}$ and $c = 5.96 \text{ \AA}$ (Wang and Tashiro, 2016). The lattice parameters from the diffractograms of PHB and

PHB-PPyI samples were calculated to be $a = 5.65 \text{ \AA}$, $b = 13.61 \text{ \AA}$ and $c = 5.86 \text{ \AA}$. The crystal size was estimated from the main diffraction peak to be 300 \AA ; and the percentage of crystallinity of both samples is 70%. Table 1 shows the crystal planes, the angular position of the diffraction peaks and the interplanar distance of the PHB crystals.



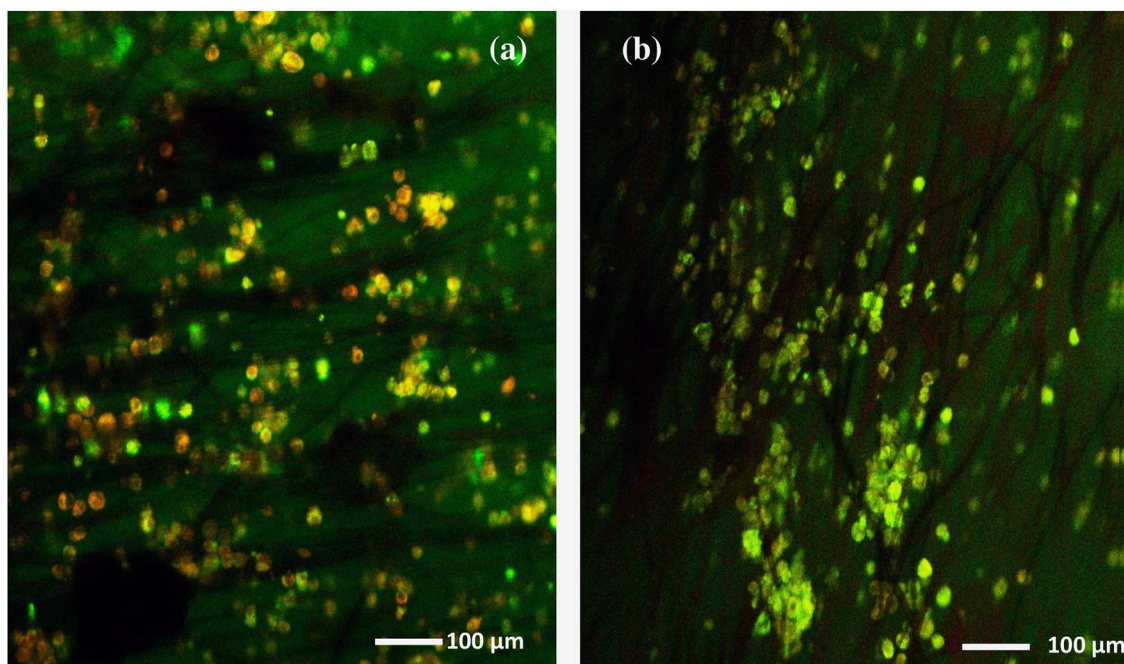


FIGURE 9 | Cell viability assay after 10 days of culture resulting images for **(A)** PHB and **(B)** PHB-PPyI scaffolds.

DSC Analysis

The thermal analysis of the scaffolds was carried out by means of differential scanning calorimetry. The DSC thermograms are shown in **Figure 5**. The melting temperature of the PHB fibers was 176°C and ΔH_m of 102.3 J/g. The degree of crystallinity is estimated at 70%, consistent with XRD results. The PHB-PPyI scaffold, in contrast, had a melting point of 172°C, lower than that of PHB. During the plasma polymerization procedure, the electric field is turned on for a few minutes before pyrrole is allowed into the reactor. The air that remains in the reactor forms a plasma which can damage the fibers. Previous studies have shown that during plasma polymerization of electrospun materials, very thin fibers disappear due to this etching (Cruz et al., 2019). This process also results in partial degradation of PHB molecules, therefore reducing the molecular weight of the PHB molecules. This is possibly the reason for the lower melting temperature that was measured in PHB-PPyI.

The DSC cooling curve (**Figure 5B**) also shows a difference in the crystallization temperature of pure PHB and PHB-PPyI. After heating to 200°C, the materials are no longer in fiber form since melting has occurred. On cooling, the PHB-PPyI sample crystallizes at a higher temperature than the PHB sample likely because PPyI fragments act as nucleation agents.

SEM Analysis

Figures 6A–C show SEM images of the electrospun PHB scaffold. The fibers are distributed over the entire observation region. **Figures 6A,B** show that the fibers were aligned by the rotation of the collecting drum, they also show the formation of beads along the fibers. The fibers alignment and a wide size distribution are more evident in **Figure 6B**. In **Figure 6C** a thick fiber with rough

surface can be observed. The roughness is likely due to the interaction of the fiber with the air during travel to the collecting cylinder as the solvents were evaporating. The fiber size distribution is shown in **Figure 6D**. The average fiber diameter is $(2.68 \pm 1.69) \mu\text{m}$.

Figures 7A–C show SEM images of the PHB-PPyI scaffold. Some fibers are fractured possibly due to their interaction with the high energy plasma. **Figure 7A** shows a panoramic view of the scaffold, and higher magnification images are shown in **Figures 7B,C**. The roughness of the coating could promote the anchorage of the cells on the fiber's surface and contribute to better cellular interaction. The PPyI coating resulted in an increase in the diameter of the fibers; the average fiber diameter was $(3.57 \pm 1.36) \mu\text{m}$. Comparing the average fiber diameter of the coated and uncoated samples indicates that the average PPyI coating thickness was 0.45 μm .

Cell Culture

Figure 8 shows optical photographs of RIN-M cells after 10 days of culture on PHB and PHB-PPyI scaffolds. The images show the frameworks of the PHB fibers and anchoring of cells on the scaffold. RIN-M cells can be seen forming cell colonies on the scaffold. Cells have also entered the scaffolding forming a 3D culture. In contrast, it is not possible to observe the internal structure of the PPyI-coated scaffold (**Figure 8B**). A monolayer of RIN-M cells can be seen growing on the edge of the PHB-PPyI scaffold. This confirms the biocompatibility of this material.

Cellular Viability

Figure 9 shows the results of the Calcein and EthD-1 cell viability assay for RIN-M cells cultured for 10 days on PHB and PHB-

PPyI. **Figure 9A** corresponds to the PHB scaffold. It is possible to identify both living and dead cells on the image. Some cell colonies are also appreciated. There are more living cells (green) than dead cells (red).

In **Figure 9B**, viable cells are observed after 10 days of cell culture on the PHB-PPyI scaffold. A large number of living cells are observed on the scaffold fibers. The cells seen in green are viable and form colonies of cells spread throughout the observation area. It is also observed that some cells anchored to the scaffold fibers. This shows that this type of scaffold allows the anchorage, growth, proliferation, and viability of this type of cells.

CONCLUSIONS

PHB electrospun scaffolds allow the anchorage, differentiation, and proliferation of RIN-M beta cells. The scaffold coated with PPyI shows a better response in cell culture. It is possible to grow RIN-M cells on these scaffolds.

In vitro cell culture tests with the RIN-M cell line showed that PHB electrospun scaffolds are biocompatible since cell adhesion and proliferation was observed. The cell viability test showed that the scaffold with best suited for beta cell culture was PHB-PPyI. This coated scaffold showed a greater number of viable cells. The materials presented in this work have the

potential to be used for treatment of diabetes mellitus in the form, for example, of an insulin producing subcutaneous patch.

DATA AVAILABILITY STATEMENT

The raw data supporting the conclusion of this article will be made available by the authors, without undue reservation.

AUTHOR CONTRIBUTIONS

EC-O participated in scaffold preparation and characterization, cell studies and wrote the manuscript. RO-V interpreted X-ray characterization. RR-T, MG-T, and SV-M aided in the preparation of the scaffolds. RG-F and OJ aided in cell culture and cell viability studies. RO and JM-C conceived the project. RO-V, RO, and JM-C were involved in writing and reviewing the manuscript.

ACKNOWLEDGMENTS

The authors thank Patricia Castillo from the UAM Iztapalapa Electron Microscopy Laboratory for electron microscopy images. JMC thanks PROMEP-SEP for the support through the “Estancias Cortas de Investigación de Integrantes de Cuerpos Académicos” program.

REFERENCES

- Ba, K, Wei, X, Ni, D, Li, N, Du, T, Wang, X, and Pan, W (2019). Chondrocyte Co-cultures with the Stromal Vascular Fraction of Adipose Tissue in Polyhydroxybutyrate/Poly-(hydroxybutyrate-co-hydroxyhexanoate) Scaffolds: Evaluation of Cartilage Repair in Rabbit. *Cell Transplant.* 28 (11), 1432–1438. doi:10.1177/0963689719861275
- Barham, P. J., Keller, A., Otun, E. L., and Holmes, P. A. (1984). Crystallization and morphology of a bacterial thermoplastic: poly-3-hydroxybutyrate. *J. Mater. Sci.* 19, 2781–2794. doi:10.1007/BF01026954
- Claudia, S., Jeyson, H., Bugallo-Casal, A., Da Silva-Candal, A., Cristina, T., Rosendo, M., et al. (2020). One-step electrospun scaffold of dual-sized gelatin/poly-3-hydroxybutyrate nano/microfibers for skin regeneration in diabetic wound. *Mater. Sci. Eng. C.* 119, 111602. doi:10.1016/j.msec.2020.111602
- Cruz, Y., Muñoz, E., Gomez-Pachón, E. Y., Morales-Corona, J., Olayo-Lortia, J., Olayo, R., et al. (2019). Electrospun PCL-protein scaffolds coated by pyrrole plasma polymerization. *J. Biomater. Sci. Polym. Ed.* 30 (10), 832–845. doi:10.1080/09205063.2019.1603338
- Daisy, E. R. A. C., Rajendran, N. K., Hourelid, N. N., Marraiki, N., Elgorban, A. M., and Rajan, M. (2020). Curcumin and Gymnema sylvestre extract loaded graphene oxide-polyhydroxybutyrate-sodium alginate composite for diabetic wound regeneration. *Reactive Funct. Polym.* 154, 104671. doi:10.1016/j.reactfunctpolym.2020.104671
- De Fronzo, R. A., Ferrannini, E., Zimmet, P., and Alberti, G. (2015). *International Textbook of Diabetes Mellitus*. Oxford, United Kingdom: Wiley-Blackwell.
- Degli Esposti, M., Federica, C., Federica, B., and Paola Fabbri, M. (2019). Highly porous PHB-based bioactive scaffolds for bone tissue engineering by in situ synthesis of hydroxyapatite. *Mater. Sci. Eng. C.* 100, 286–296. doi:10.1016/j.msec.2019.03.014
- Furukawa, T., Sato, H., Murakami, R., Zhang, J., Noda, I., Ochiai, S., and Ozaki, Y. (2006). Raman microspectroscopy study of structure, dispersibility, and crystallinity of poly(hydroxybutyrate)/poly(l-lactic acid) blends. *Polymer* 47, 3132–3140. doi:10.1016/j.polymer.2006.03.010
- Maryam, M, and Saeed, S (2020). Physical, mechanical and biological performance of PHB-Chitosan/MWCNTs nanocomposite coating deposited on bioglass based scaffold: Potential application in bone tissue engineering. *Int. J. Biol. Macromol.* 152, 645–662. doi:10.1016/j.ijbiomac.2020.02.266
- Michael, B., Czado, W., Thomas, F., Andreas, S., Michael, H., Martin, S., et al. (2001). Nanostructured fibers via electrospinning. *Adv. Mater.* 13 (1), 70–72. doi:10.1002/1521-4095(200101)13:1<70::AID-ADMA70>3.0.CO;2-H
- Naderi, P., Zarei, M., Karbasi, S., and Salehi, H. (2020). Evaluation of the Effects of keratin on Physical, Mechanical and Biological Properties of Poly (3-hydroxybutyrate) Electrospun Scaffold: Potential Application in Bone Tissue Engineering. *Eur. Polym. J.* 124, 109502. doi:10.1016/j.eurpolymj.2020.109502
- Nahideh, A., Del Bakhshayesh, A. R., Soodabeh, D., and Akbarzadeh, A. (2019). Common biocompatible polymeric materials for tissue engineering and regenerative medicine. *Mater. Chem. Phys.* 242, 122528. doi:10.1016/j.matchemphys.2019.122528
- O'Brien, F. J. (2011). Biomaterials and scaffolds for tissue engineering. *Materials Today* 14, 88–95. doi:10.1016/S1369-7021(11)70058-X
- Ogurtsova, K., da Rocha Fernandes, J.D., Huang, Y., Linnenkamp, U., Guariguata, L., Cho, N. H., et al. (2018). IDF diabetes atlas: Global estimates of diabetes prevalence for 2017 and projections for 2045. *Diabetes Res. Clin. Pract.* 138, 271–281. doi:10.1016/j.diabres.2018.02.023
- Ramírez-Fernández, O., Godínez, R., Morales, J., Gómez-Quiroz, L., Gutiérrez-Ruiz, M. C., Zuñiga-Aguilar, E., and Olayo, R. (2012). Glow discharge plasma modified surfaces for hepatic co-culture models. *Rev. Mex. Ing. Biomed.* 33, 127–135.
- Ramírez-Fernández, O., Godínez, R., Morales, J., Gómez-Quiroz, L., Gutiérrez-Ruiz, M. C., Zuñiga-Aguilar, E., and Olayo, R., et al. (2015). Hepatocyte culture in a radial-flow bioreactor with plasma polypyrrole coated scaffolds. *Biocell* 39, 9–14. doi:10.32604/biocell.2015.39.009
- Ruiz Velasco, G., Martínez-Flores, F., Morales-Corona, J., Olayo-Valles, R., and Olayo, R. (2017). Polymeric scaffolds for skin. *Macromol. Symp.* 374, 1600133. doi:10.1002/MASY.201600133
- Sadeghi, D., Karbasi, S., Razavi, S., Mohammadi, S., Shokrgozar, M. A., and Bonakdar, S. (2016). Electrospun poly(hydroxybutyrate)/chitosan blend

- fibrous scaffolds for cartilage tissue engineering. *J. Appl. Polym. Sci.* 133, 44171. doi:10.1002/app.44171
- Socrates, G. (2001). *Infrared and Raman characteristic group frequencies; tables and charts*. 3rd Edn. Chichester, United Kingdom: John Wiley and Sons.
- Toloua, E. B., Karbasi, S., Salehi, H., and Rafienia, M. (2019). Evaluation of mechanical properties and cell viability of poly (3-hydroxybutyrate)-chitosan/Al₂O₃ nanocomposite scaffold for cartilage tissue engineering. *J. Med. Signals Sens* 9 (2), 111–116. doi:10.4103/jmss.JMSS_56_18
- Toloua, E. B., Karbasi, S., Salehi, H., and Rafienia, M. (2019). Potential of an electrospun composite scaffold of poly (3-hydroxybutyrate)-chitosan/alumina nanowires in bone tissue engineering applications. *Mater. Sci. Eng. C.* 99, 1075–1091. doi:10.1016/j.msec.2019.02.062
- Tsuyoshi, F., Sato, H., Murakami, R., Zhang, J., Noda, I., Shukichi, O., et al. (2006). Raman microspectroscopy study of structure, dispersibility, and crystallinity of poly(hydroxybutyrate)/poly(L-lactic acid) blends. *Polymer* 47 (9), 3132–3140. doi:10.1016/j.polymer.2006.03.010
- Vazquez Ortega, M., Ortega, M., Morales, J., Olayo, M. G., Cruz, G. J., and Olayo, R. (2014). Core-shell polypyrrole nanoparticles obtained by atmospheric pressure plasma polymerization. *Polym. Int.* 63, 2023–2029. doi:10.1002/PI.4756
- Wang, H., and Tashiro, K. (2016). Reinvestigation of crystal structure and intermolecular interactions of biodegradable poly(3-hydroxybutyrate) α -form and the prediction of its mechanical property. *Macromolecules* 49, 581. doi:10.1021/acs.macromol.5b02310
- World Health Organization and International Diabetes Federation(2006). *Definition and diagnosis of diabetes mellitus and intermediate hyperglycaemia*. Geneva, Switzerland: World Health Organization and International Diabetes Federation.
- Zamanifard, M., Khorasani, M. T., Daliri, M., and Parvazinia, M. (2020). Preparation and modeling of electrospun polyhydroxybutyrate/polyaniline composite scaffold modified by plasma and printed by an inkjet method and its cellular study. *J. Biomater. Sci. Polym. Edition* 31 (12), 1515–1537. doi:10.1080/09205063.2020.1764162
- Zhuikov, V. A., Akoulina, E. A., Chesnokova, D. V., Wenhao, Y., Makhina, T. K., Demyanova, I. V., et al. (2021). The growth of 3T3 fibroblasts on PHB, PLA and PHB/PLA blend films at different stages of their biodegradation in vitro. *Polymers* 13, 108. doi:10.3390/polym13010108
- Zuñiga Aguilar, E., Olayo, R., Ramirez-Fernández, O., Morales, J., and Godínez, R. (2014). Nerve cells culture from lumbar spinal cord on surfaces modified by plasma pyrrole polymerization. *J. Biomater. Sci. Polym. Edition* 25, 729–747. doi:10.1080/09205063.2014.898124
- Zviagin, A. S., Chernozem, R. V., Surmeneva, M. A., Pyeon, M., Frank, M., Ludwig, T., et al. (2019). Enhanced piezoelectric response of hybrid biodegradable 3D poly(3-hydroxybutyrate) scaffolds coated with hydrothermally deposited ZnO for biomedical applications. *Eur. Polym. J.* 117, 272–279. doi:10.1016/j.eurpolymj.2019.05.016

Conflict of Interest: The authors declare that the research was conducted in the absence of any commercial or financial relationships that could be construed as a potential conflict of interest.

Copyright © 2021 Cortés-Ortiz, Olayo-Valles, Rodríguez-Talavera, González-Torres, Vargas-Muñoz, Olayo, Godínez-Fernández, Uribe Juárez and Morales-Corona. This is an open-access article distributed under the terms of the Creative Commons Attribution License (CC BY). The use, distribution or reproduction in other forums is permitted, provided the original author(s) and the copyright owner(s) are credited and that the original publication in this journal is cited, in accordance with accepted academic practice. No use, distribution or reproduction is permitted which does not comply with these terms.